Supplementary material for:

A comparative Study of Structure and Bonding in Heavier Pnictinidene Complexes [(ArE)M(CO)$_n$] (E = As, Sb and Bi; M = Cr, Mo, W and Fe).

Iva Vránová,[a] Vít Kremláček,[a] Milan Erben,[a] Jan Turek,[b,] Roman Jambor,[a] Aleš Růžička,[a] Mercedes Alonso,[b] Libor Dostál[a,*]*

*E-mail: libor.dostal@upce.cz, jturek@vub.ac.be

Table of contents:

1) X-ray diffraction analyses and Table S1 and Figures S1-S10 **page S2**

2) Details for IR and Raman spectroscopy **page S9**

3) Computational details **page S12**

4) Computational results **page S13**

5) References **page S16**

1) X-ray diffraction analyses

Suitable single crystals of the studied compounds were mounted on glass fiber and measured on the four-circle diffractometer KappaCCD with a CCD area detector by monochromatized MoKα radiation (λ = 0.71073 Å). The corresponding crystallographic data are given in Table S1. The numerical[S1] absorption correction from the crystal shape was applied for all crystals. The structures were solved by the direct method (SIR92[S2]) and refined by a full matrix least squares procedure based on F^2 (SHELXL97[S3]). Hydrogen atoms were mostly localized on a difference Fourier map, however, to ensure a uniform crystal treatment, all hydrogen atoms were recalculated into idealized positions (riding model) and assigned temperature factors *Uiso*(H) = 1.2*Ueq*(pivot atom) or of 1.5*Ueq* for the methyl moiety with C-H = 0.96 Å, 0.98, and 0.93 Å for methyl, methine and hydrogen atoms in aromatic rings, respectively. The structure of **2c** contains a disorder of *t*-butyl and two carbonyl groups, which were split into two positions with occupancy for each carbon atom of *t*-butyl group of about 1:1 and 1:1 and 3:2 for carbonyl groups, respectively. This disorder was treated with SHELXL97 software.[S3] The same problem was found in the structure of **3b** where *t*Bu and two carbonyl groups were split into two pairs of positions with the occupancy 3:2 (*t*Bu) and 1:1 (for both CO groups) and this problem was treated with the same SHELXL97 software as in the previous case.[S3] There are residual electron maxima and cavities within the unit cell originating from the disordered toluene in the structures of **2a** and **2b**. PLATON/SQUEZZE[S4] was used to correct the data for the presence of a disordered solvent. A potential solvent volume of 744 $Å^3$ was found in the structure of **2a** and 740 $Å^3$ of **2b**. 200 and 128 electrons per unit cell worth of scattering were located in the void. The calculated stoichiometry of the solvent was calculated to be four or two molecules of toluene per unit cell. PLATON/SQUEZZE[S4] was used to correct the data for the presence of disordered toluene in the structure of **1a** resulting in the modeling of one half of toluene molecule per one molecule

of **1a**. In this structure the thermal ellipsoid of the C10 atom was improved by standard ISOR instruction implemented in the SHELXL97 software.[S3] Crystallographic data for the structural analysis were deposited with the Cambridge Crystallographic Data Centre, CCDC nos. 1515224-1515233. Copies of this information may be obtained free of charge from The Director, CCDC, 12 Union Road, Cambridge CB2 1EY, UK (Fax: +44-1223-336033; e-mail: deposit@ccdc.cam.ac.uk or www: http://www.ccdc.cam.ac.uk).

Table S1. Crystallographic data for the studied compounds.

	1a	**1d**	**2a**	**2b**
chemical formula	$C_{21}H_{23}AsCrN_2O_5$. 0.5(C_7H_8)	$C_{20}H_{23}AsFeN_2O_4$	$C_{21}H_{23}CrN_2O_5Sb$. 0.5(C_7H_8)	$C_{21}H_{23}MoN_2O_5Sb$. 0.25(C_7H_8)
cryst syst	monoclinic	monoclinic	monoclinic	monoclinic
space group	*C2/c*	*Cc*	*C2/c*	*C2/c*
a[Å]	28.0370(3)	13.9922(4)	28.4024(6)	28.7432(3)
b[Å]	9.3332(4)	16.2860(2)	9.3490(2)	9.4385(7)
c[Å]	19.4852(3)	9.5112(3)	19.5303(5)	19.6321(3)
α[°]	90	90	90	90
β[°]	95.871(2)	102.863(5)	95.652(4)	96.060(2)
γ[°]	90	90	90	90
Z	8	4	8	8
μ[mm^{-1}]	1.782	2.295	1.504	1.525
D_x [Mg m^{-3}]	1.457	1.528	1.553	1.565
cryst size [mm]	0.59x0.41x0.39	0.50×0.44×0.10	0.30x0.23x0.05	0.35×0.25×0.09
θ range, [deg]	1-27.5	1-27.4	1-27.5	1-27.5
T_{min}, T_{max}	0.512, 0.655	0.493, 0.845	0.775, 0.927	0.734, 0.886
no. of reflns measd	16 519	14 579	20 016	25 340
no. of unique reflns, R_{int}	5351, 0.033	4586, 0.022	5807, 0.033	5821, 0.020
no. of obsd reflns	4006	4432	4502	5160
no. of params	271	253	271	271
S all data	1.169	1.090	1.099	1.009
final R indices [$I>2\sigma(I)$]	0.058	0.018	0.028	0.021
wR2 indices (all data)	0.113	0.040	0.053	0.053
Δρ, max., min. [e $Å^{-3}$]	1.679, -2.387	0.248, -0.306	0.332, -0.577	0.350, -0.421

Table S1(continue). Crystallographic data for **10a - 12**.

	2c	**2d**	**3a**	**3b**
chemical formula	$C_{21}H_{23}N_2O_5SbW$	$C_{20}H_{23}FeN_2O_4Sb$	$2(C_{21}H_{23}BiCrN_2O_5).C_7H_8$	$C_{21}H_{23}BiMoN_2O_5$
cryst syst	Triclinic	monoclinic	orthorhombic	Triclinic
space group	*P-1*	*P21/c*	$P2_12_12_1$	*P-1*
a[Å]	10.5080(11)	10.9560(8)	19.3042(13)	10.5700(7)
b[Å]	10.5261(16)	9.9450(4)	19.3039(14)	10.6180(8)
c[Å]	11.4350(13)	19.8771(12)	13.576(3)	11.4101(8)
α[°]	70.486(7)	90	90	70.472(7)
β[°]	89.138(10)	96.737(5)	90	89.817(7)
γ[°]	78.361(8)	90	90	78.893(6)
Z	2	4	4	2
μ[mm^{-1}]	6.121	1.975	7.413	7.998
D_x [Mg m^{-3}]	1.963	1.646	1.813	1.934
cryst size [mm]	0.28×0.17×0.11	0.43×0.40×0.40	0.55x0.49x0.10	0.57×0.54×0.15
θ range, [deg]	1-27.5	1-27.5	1-27.5	1-27.5
T_{min}, T_{max}	0.339, 0.679	0.498, 0.571	0.085, 0.493	0.063, 0.356
no. of reflns measd	20 829	16 165	38 570	25 088
no. of unique reflns, R_{int}	5337, 0.053	4662, 0.020	11036, 0.047	5402, 0.033
no. of obsd reflns	4996	4290	9184	5070
no. of params	295	487	604	295
S all data	1.061	1.154	1.170	1.109
final R indices [$I>2\sigma(I)$]	0.044	0.020	0.037	0.028
wR2 indices (all data)	0.114	0.046	0.069	0.068
Δρ, max., min. [e $Å^{-3}$]	3.563, -4.001	0.480, -0.634	1.833, -1.623	1.475, -3.047

Table S1(continued). Crystallographic data for **13**.

	3c	**3d**
chemical formula	$2(C_{21}H_{23}BiN_2O_5W).C_7H_8$	$C_{20}H_{23}BiFeN_2O_4$
cryst syst	orthorhombic	monoclinic
space group	$P2_12_12_1$	*P21/c*
a[Å]	19.4793(16)	11.1360(10)
b[Å]	19.4789(13)	11.5650(10)
c[Å]	13.5431(16)	18.6181(13)
α[°]	90	90
β[°]	90	112.958(6)
γ[°]	90	90
Z	4	4
μ[mm^{-1}]	11.349	8.643
D_x [Mg m^{-3}]	2.126	1.866
cryst size [mm]	0.39×0.31×0.20	0.32×0.29×0.29
θ range, [deg]	1-27.5	1-27.5
T_{min}, T_{max}	0.113, 0.211	0.222, 0.326
no. of reflns measd	21 522	21 097
no. of unique reflns, R_{int}	11091, 0.062	4989, 0.041
no. of obsd reflns	10306	4132
no. of params	604	253
S all data	1.108	1.139
final R indices [$I>2\sigma(I)$]	0.045	0.032
wR2 indices (all data)	0.108	0.0886
Δρ, max., min. [e $Å^{-3}$]	3.613, -2.686	2.338, -1.510

$R_{int} = \sum | F_o^2 - F_{o,mean}^2 | / \sum F_o^2$, GOF = $[\sum(w(F_o^2 - F_c^2)^2)/(N_{diffrs} - N_{params})]^{½}$ for all data, $R(F) = \sum | |F_o| - |F_c| | / \sum |F_o|$ for observed data, $wR(F^2) = [\sum(w(F_o^2 - F_c^2)^2)/(\sum w(F_o^2)^2)]^{½}$ for all data.

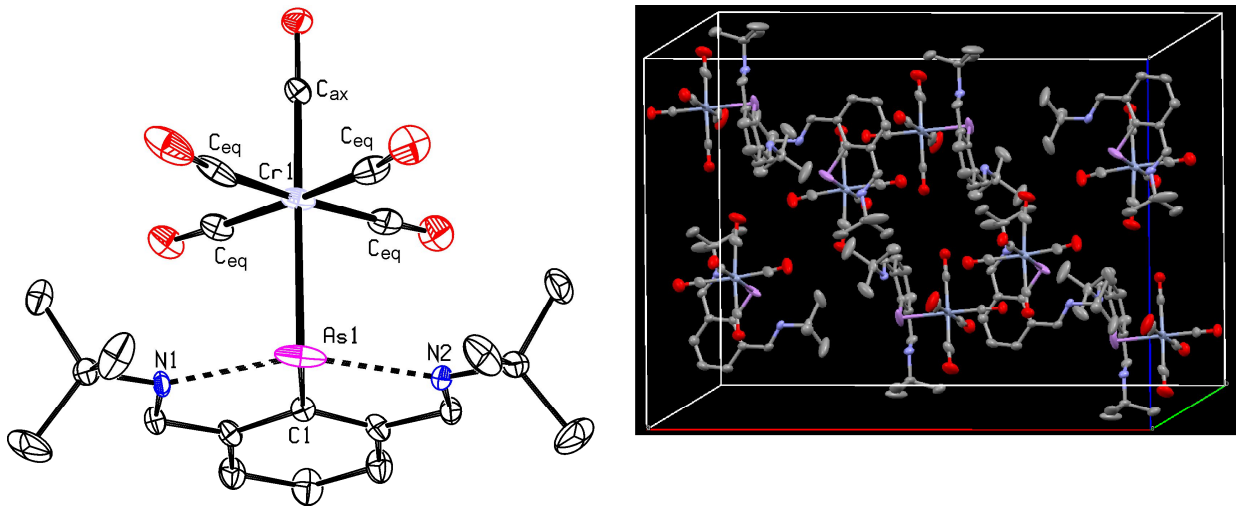

Figure S1: Molecular structure of **1a** together with a packing in the unit cell.

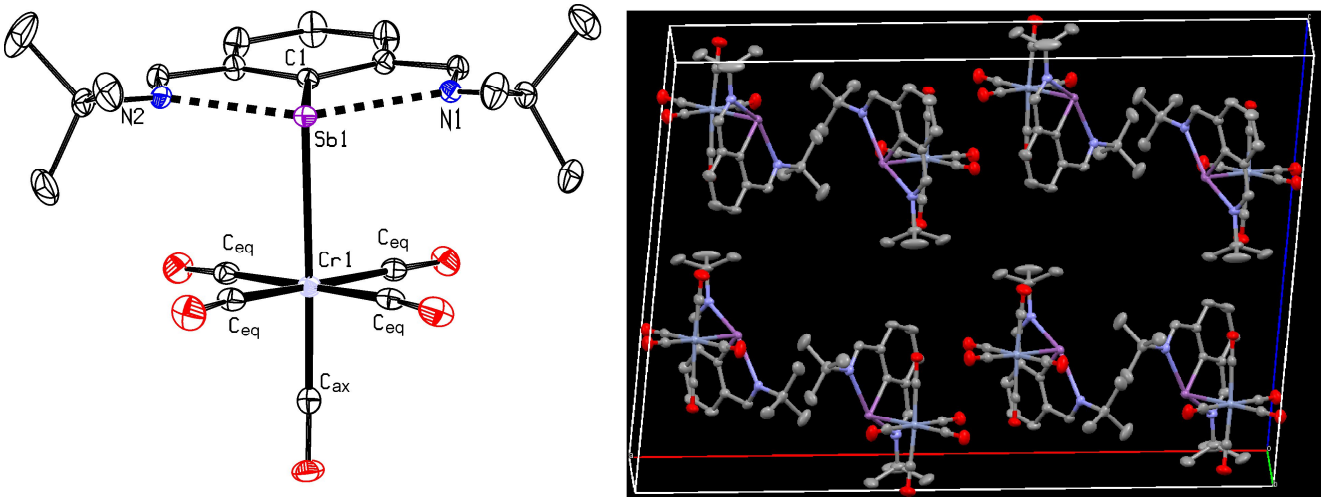

Figure S2: Molecular structure of **2a** together with a packing in the unit cell.

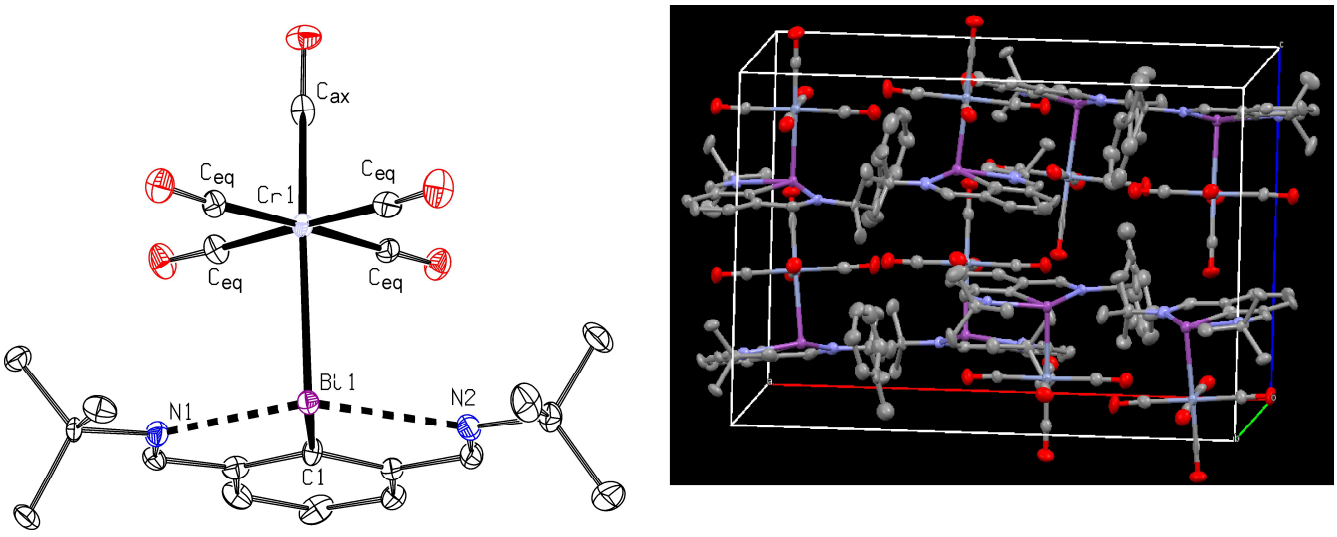

Figure S3: Molecular structure of **3a** together with a packing in the unit cell.

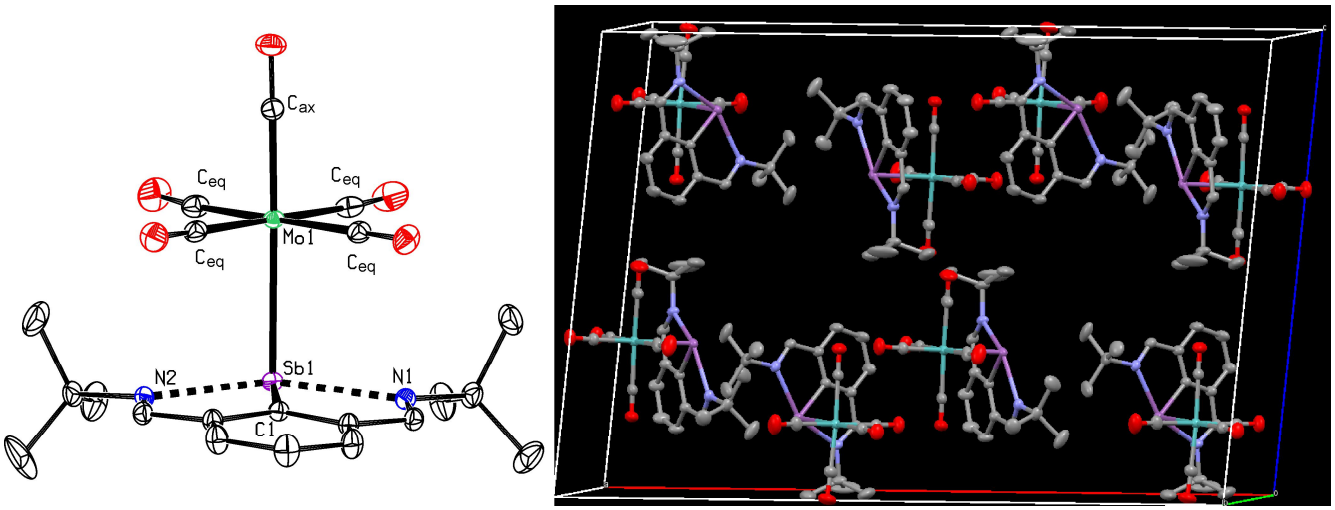

Figure S4: Molecular structure of **2b** together with a packing in the unit cell.

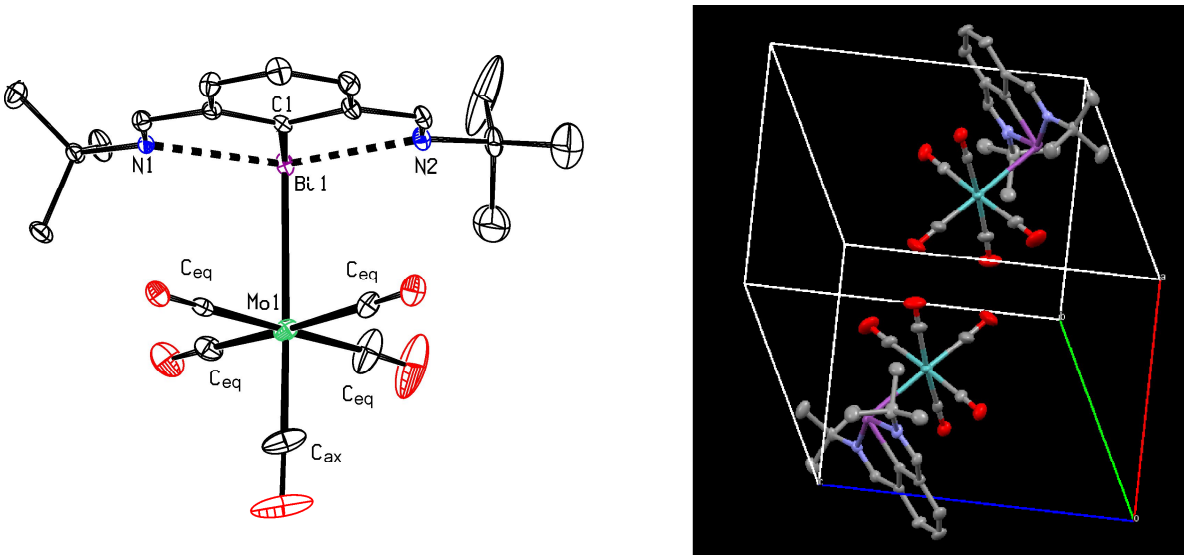

Figure S5: Molecular structure of **3b** together with a packing in the unit cell.

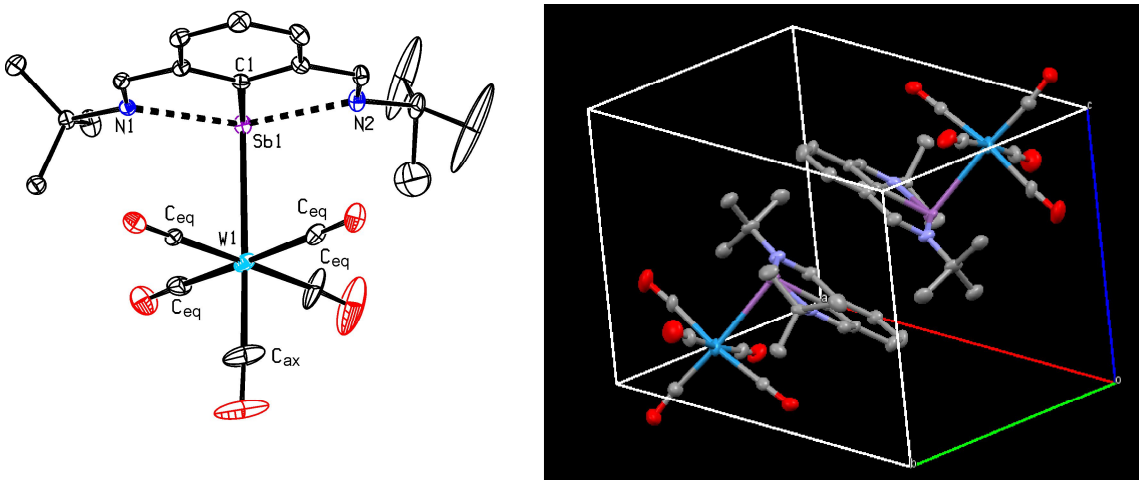

Figure S6: Molecular structure of **2c** together with a packing in the unit cell.

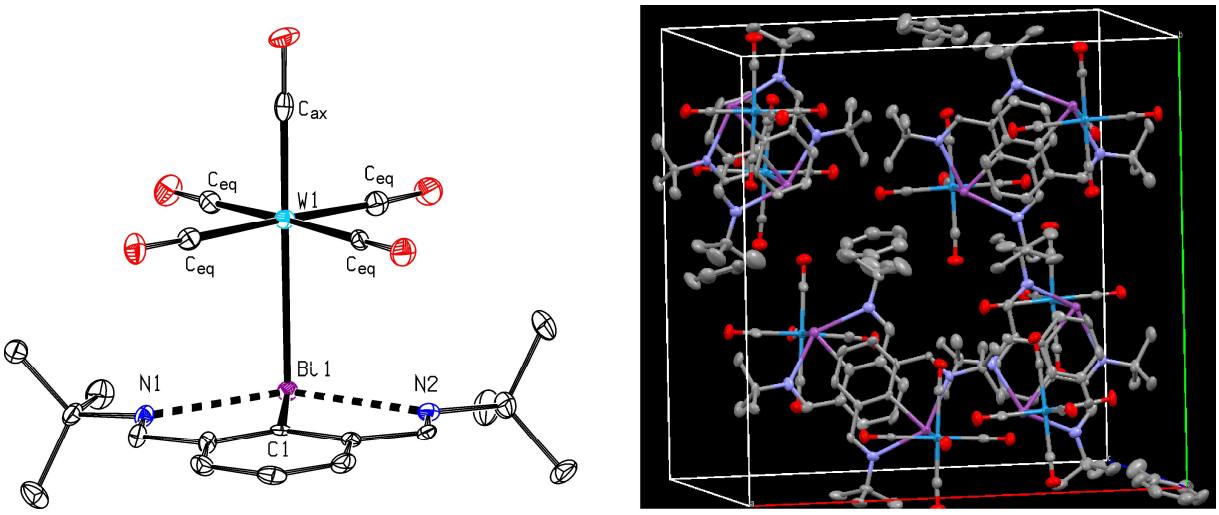

Figure S7: Molecular structure of **3c** together with a packing in the unit cell.

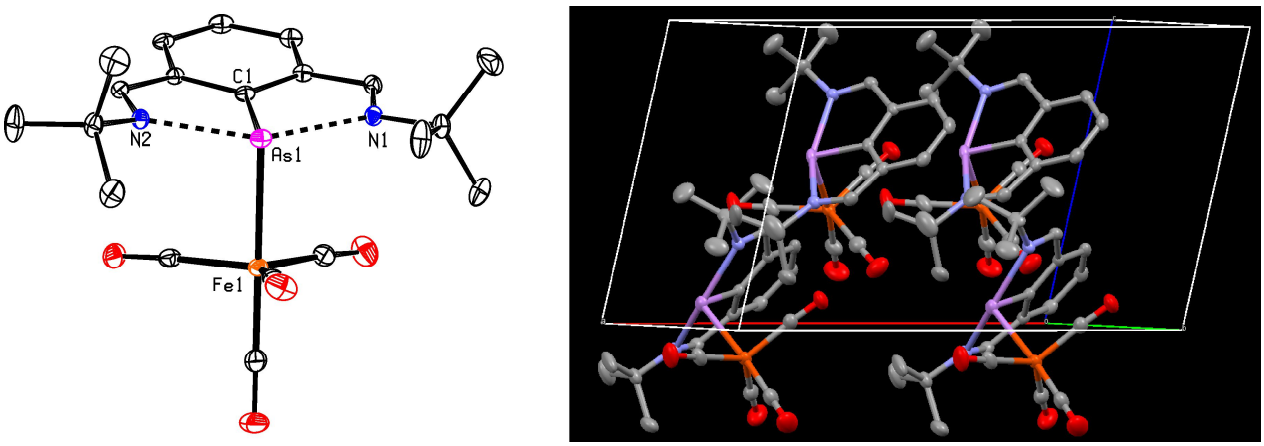

Figure S8: Molecular structure of **1d** together with a packing in the unit cell.

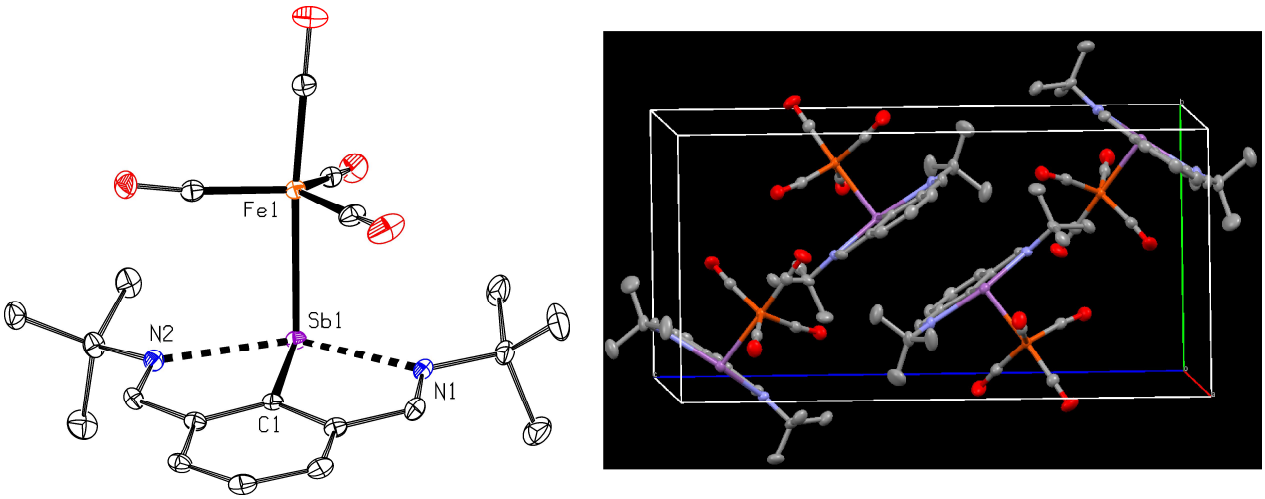

Figure S9: Molecular structure of **2d** together with a packing in the unit cell.

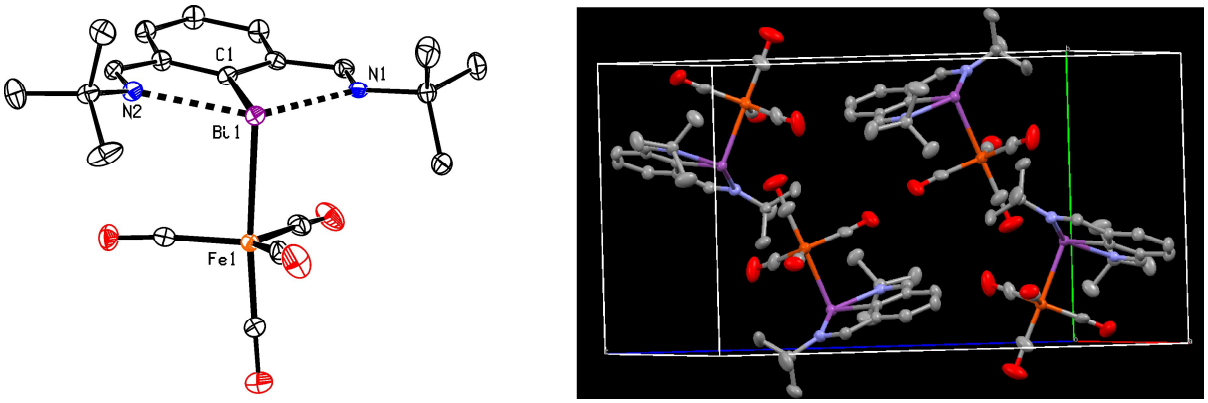

Figure S10: Molecular structure of **3d** together with a packing in the unit cell.

2) Details for IR and Raman spectroscopy

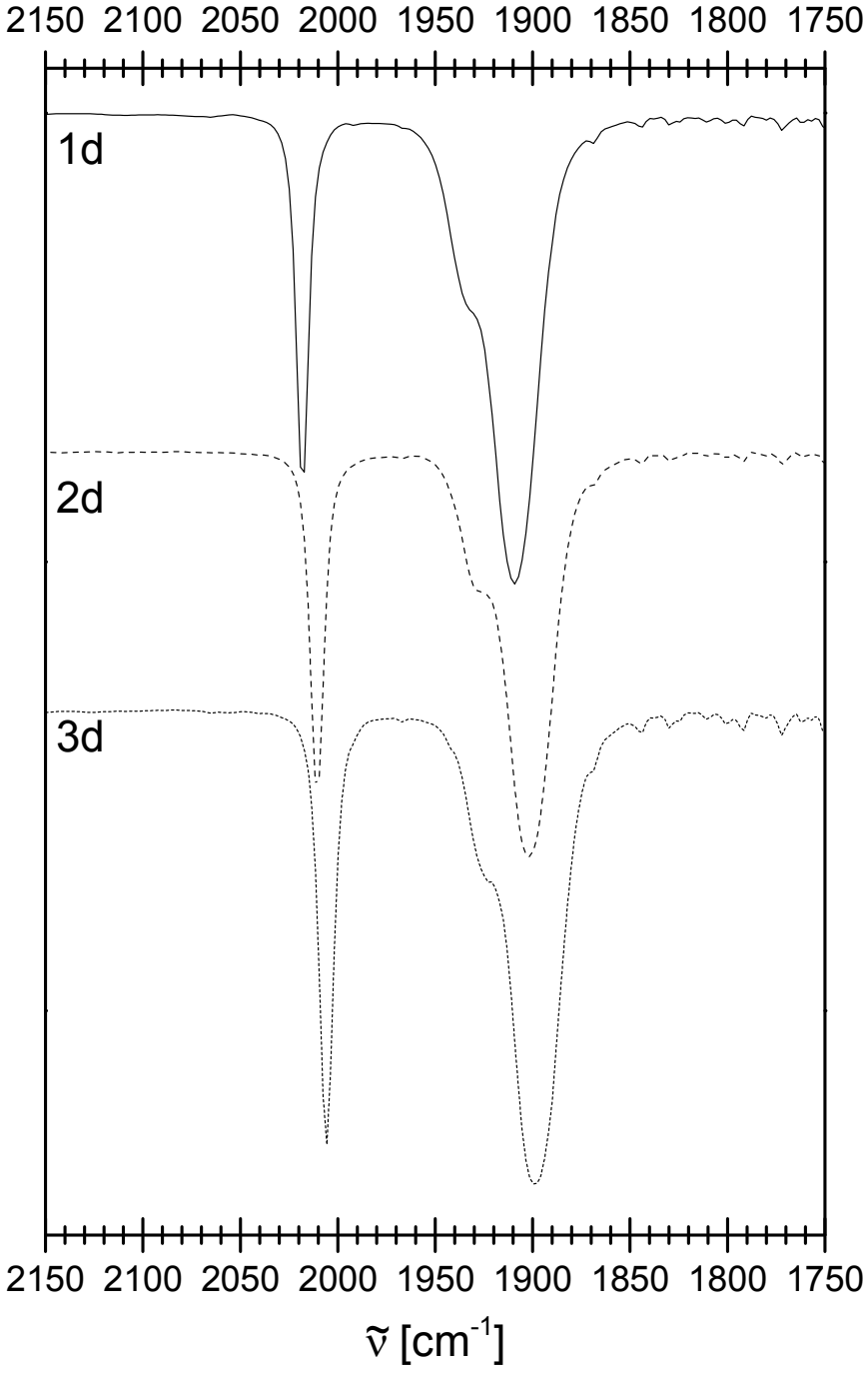

Figure S11: Solution IR spectra of $ArEFe(CO)_4$ complexes in the region of ν_{CO} stretching vibrations.

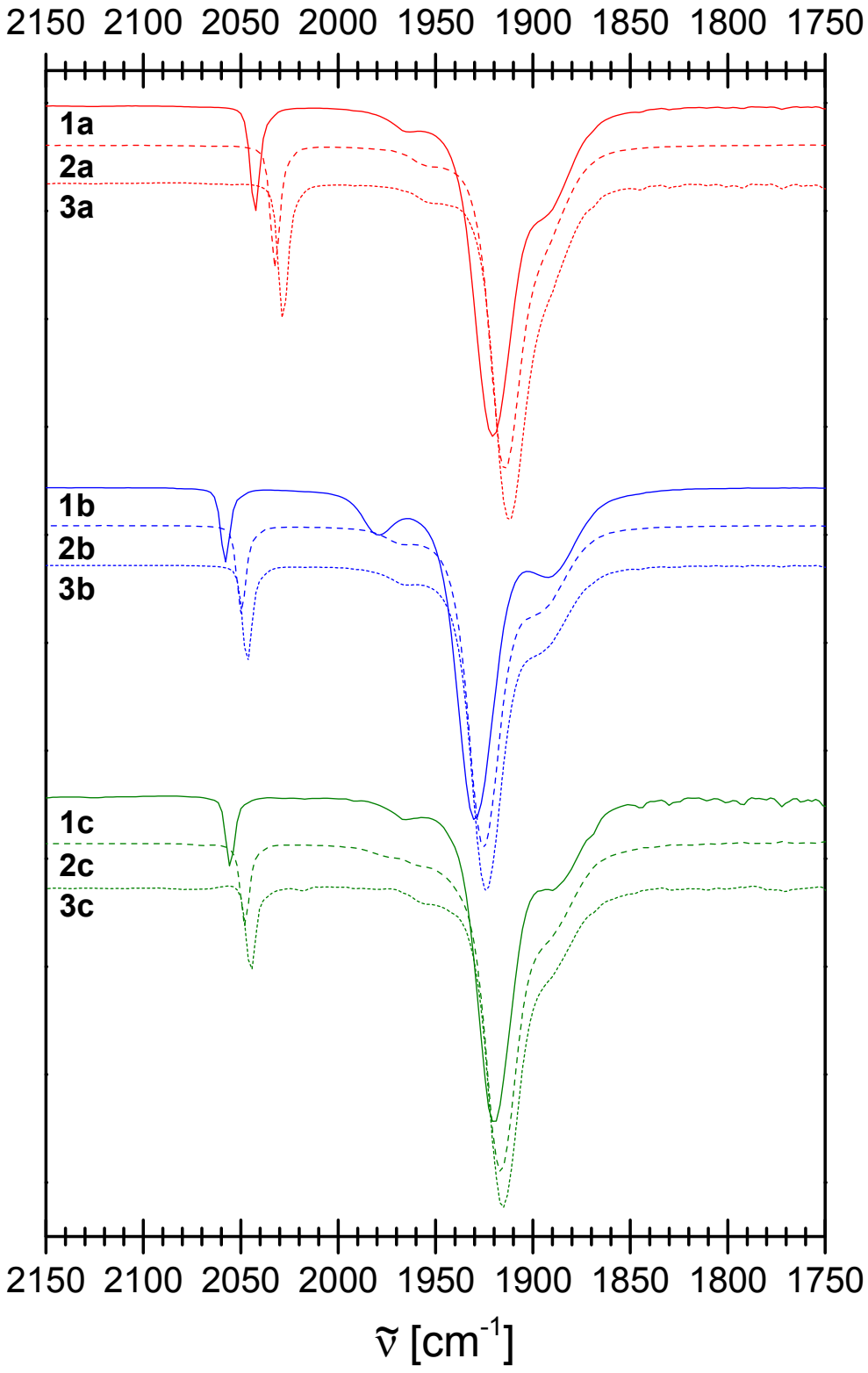

Figure S12: Solution IR spectra of $ArEM(CO)_5$ complexes in the region of ν_{CO} stretching vibrations.

Table S2: Infrared CO stretching frequencies (cm^{-1}) for $ArEM(CO)_5$ derivatives measured in hexane solutions.

$ArEM(CO)_5$	A_1^{eq}	B_1	E	A_1^{ax}
1a (E = As, M = Cr)	2044	*n.o.*	1924	1912
2a (E = Sb, M = Cr)	2034	*n.o.*	1921	1916
3a (E = Bi, M = Cr)	2031	*n.o.*	1921	1914
1b (E = As, M = Mo)	2058	1956	1931	1914
2b (E = Sb, M = Mo)	2050	*n.o.*	1928	1919
3b (E = Bi, M = Mo)	2048	*n.o.*	1927	1919
1c (E = As, M = W)	2051	1962	1922	1911
2c (E = Sb, M = W)	2049	*n.o.*	1921	1918
3c (E = Bi, M = W)	2048	*n.o.*	1921	1917

3) Computational details

All calculations were carried out using Density Functional Theory (DFT) as implemented in the Gaussian09 quantum chemistry program.[S5] Geometry optimizations were carried out at the M06/cc-pVDZ[S6] level of theory (for heavier atoms - As, Sb, Bi, Mo and W - the cc-pVDZ-PP[S7] basis set including small-core relativistic pseudopetentials that account also for relativistic effects. The electronic energies were re-evaluated by additional single point calculations on each of all optimized geometries using the triple-ζ-quality cc-pVTZ(-PP) basis set. Analytical vibrational frequencies within the harmonic approximation were computed with the cc-pVDZ basis set to confirm a proper convergence to well-defined minima or saddle points on the potential energy surface. The subsequent NBO analysis[S8] and calculation of Wiberg bond indices[S9] were performed at the M06/cc-pVTZ(-PP) level.

4) Computational results

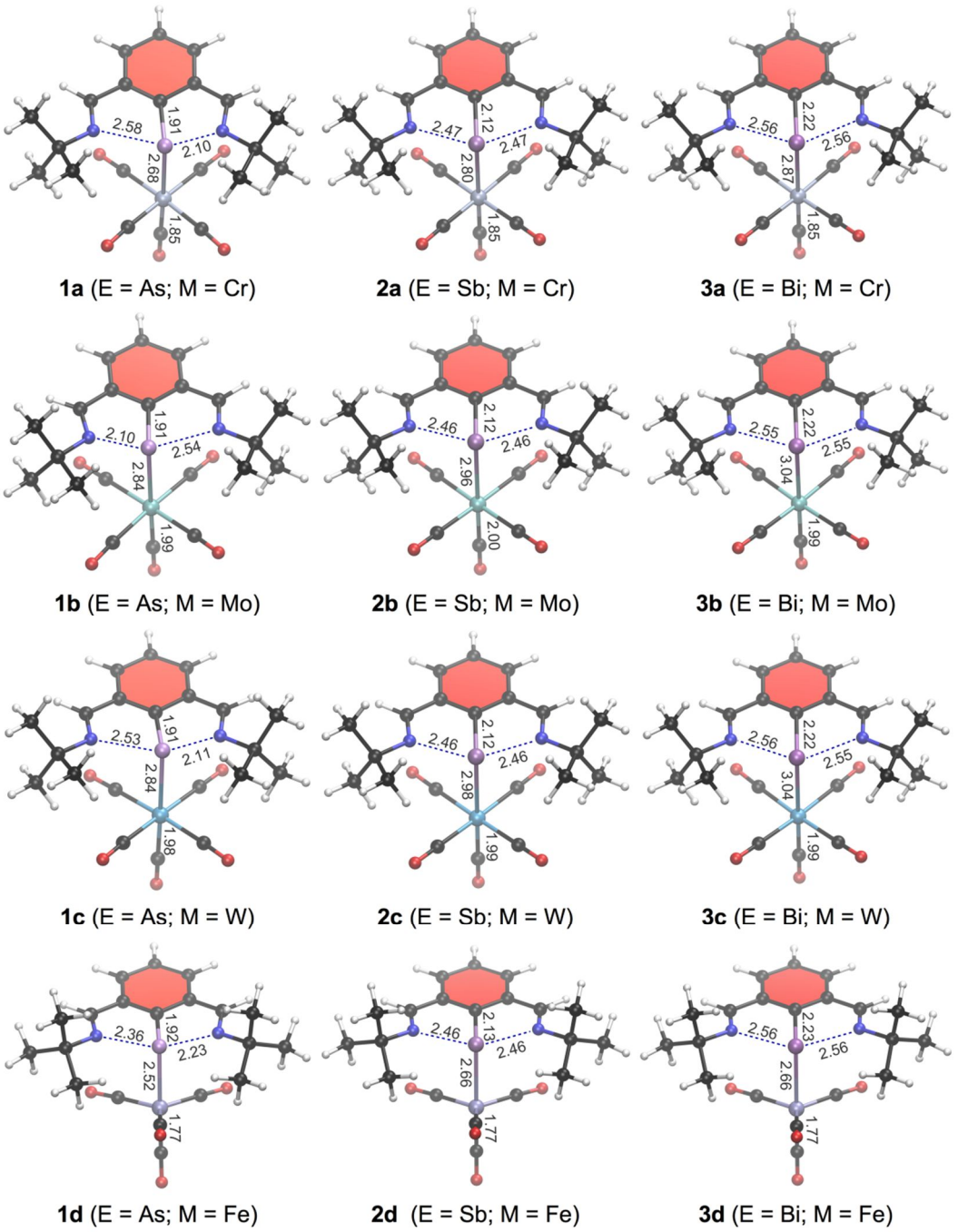

Figure S13: M06/cc-pVDZ(-PP) optimized geometries of compounds **1a-3d** along with selected distances (in Å).

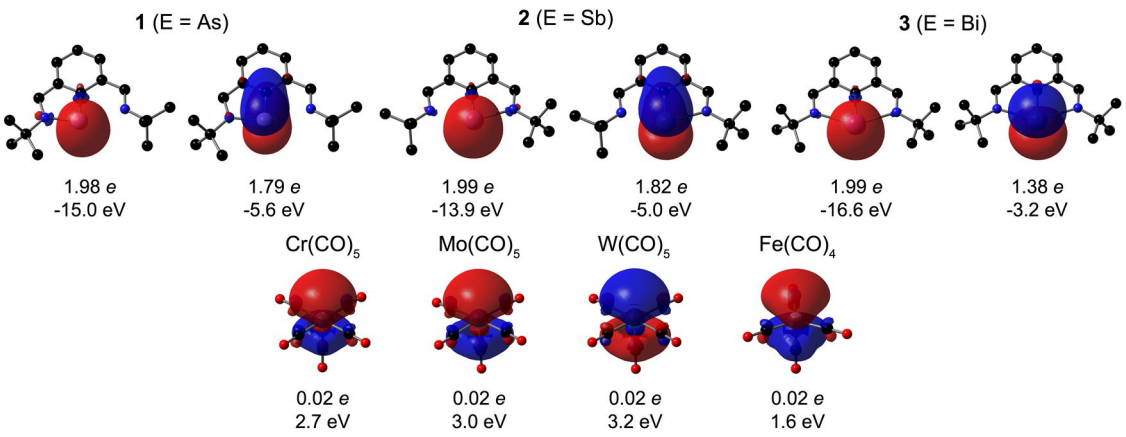

Figure S14: Relevant NBOs (isosurface 0.03 a.u.) showing the σ- and π-type lone pair orbitals on the pnictogen center in pnictinidenes **1-3** and the empty orbital on the TM center in $M(CO)_n$ (Hydrogen atoms are omitted for clarity). NBO populations and orbital energies are also displayed.

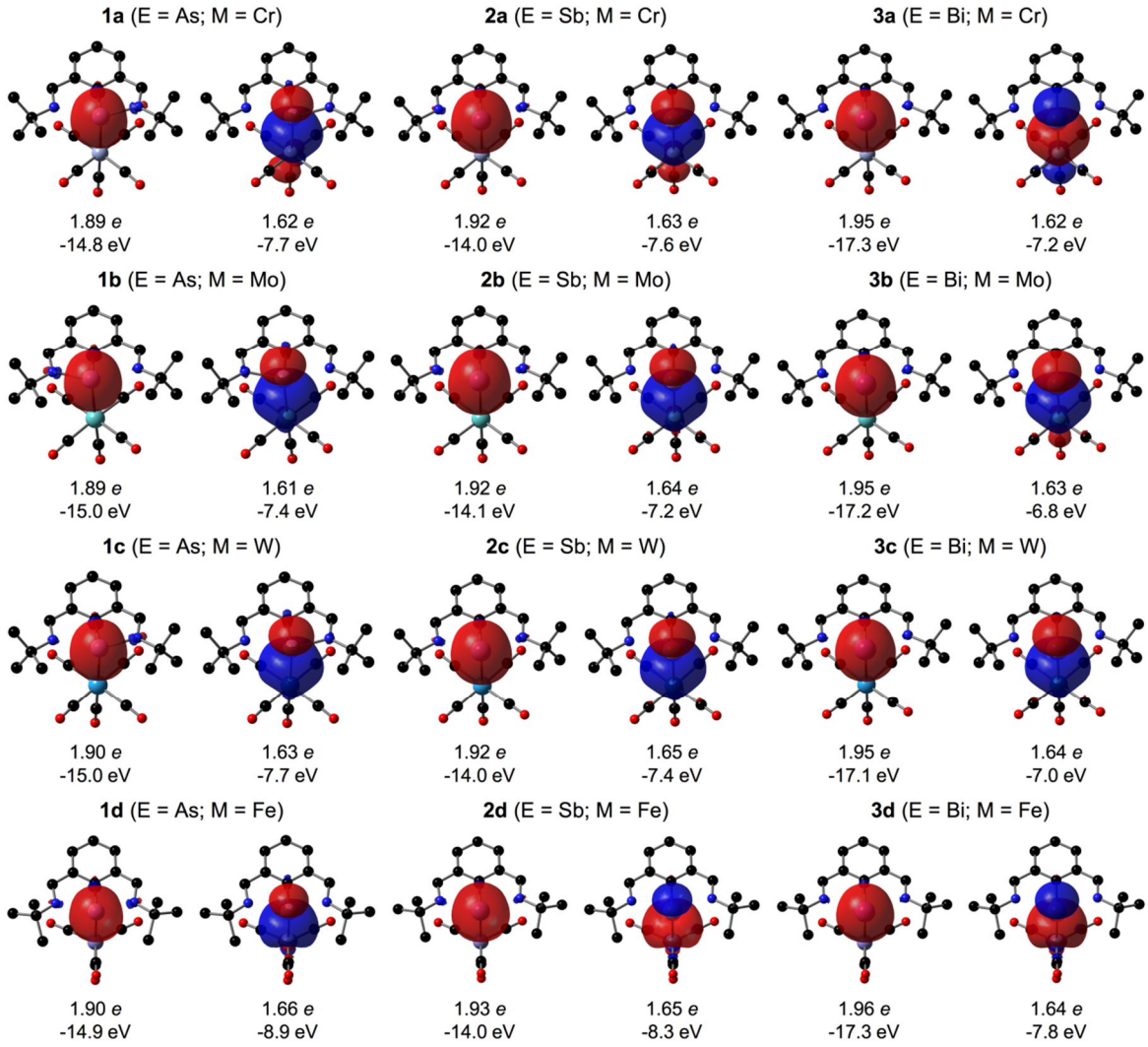

Figure S15: Relevant NBOs (isosurface 0.03 a.u.) showing the *s*-type lone pair on the pnictogen center and E-M σ-bond in **1a-3d** (Hydrogen atoms are omitted for clarity). NBO populations and orbital energies are also displayed.

5) References

[S1] P. Coppens, In *Crystallographic Computing* F.R. Ahmed, S.R. Hall and C.P. Huber, Eds; Copenhagen, Munksgaard, 1970; pp 255.

[S2] A. Altomare, G. Cascarone, C. Giacovazzo, A. Guagliardi, M.C. Burla, G. Polidori and M. Camalli, *J. Appl. Crystallogr.*, 1994, **27**, 1045-1050.

[S3] G.M. Sheldrick, G.M. SHELXL-97, University of Göttingen: Göttingen, 2008.

[S4] A.L. Spek, *Acta Cryst.*, 2015, **C71**, 9-18.

[S5] Frisch, M.J.; Trucks, G.W.; Schlegel, H.B.; Scuseria, G.E.; Robb, M.A.; Cheeseman, J. R.; Scalmani, G.; Barone, V.; Mennucci, B.; Petersson, G.A.; Nakatsuji, H.; Caricato, M.; Li, X.; Hratchian, H.P.; Izmaylov, A.F.; Bloino, J.; Zheng, G.; Sonnenberg, J.L.; Hada, M.; Ehara, M.; Toyota, K.; Fukuda, R.; Hasegawa, J.; Ishida, M.; Nakajima, T.; Honda, Y.; Kitao, O.; Nakai, H.; Vreven, T.; Montgomery, Jr., J.A.; Peralta, J.E.; Ogliaro, F.; Bearpark, M.; Heyd, J.J.; Brothers, E.; Kudin, K.N.; Staroverov, V.N.; Kobayashi, R.; Normand, J.; Raghavachari, K.; Rendell, A.; Burant, J.C.; Iyengar, S.S.; Tomasi, J.; Cossi, M.; Rega, N.; Millam, J.M.; Klene, M.; Knox, J.E.; Cross, J.B.; Bakken, V.; Adamo, C.; Jaramillo, J.; Gomperts, R.; Stratmann, R.E.; Yazyev, O.; Austin, A.J.; Cammi, R.; Pomelli, C.; Ochterski, J.W.; Martin, R.L.; Morokuma, K.; Zakrzewski, V.G.; Voth, G.A.; Salvador, P.; Dannenberg, J.J.; Dapprich, S.; Daniels, A.D.; Farkas, Ö.; Foresman, J.B.; Ortiz, J.V.; Cioslowski, J.; Fox, D.J. *Gaussian 09, Revision B.01*, Gaussian, Inc., Wallingford CT, 2009.

[S6] a) Y. Zhao and D.G. Truhlar, *Theor. Chem. Acc.*, 2008, **120**, 215-241; b) T.H. Dunning, *J. Chem. Phys.*, 1989, **90**, 1007-1023; c) D.E. Woon and T.H. Dunning, *J. Chem. Phys.*, 1993, **99**, 1358-1371.

[S7] a) K.A. Peterson, *J. Chem. Phys.*, 2003, **119**, 11099-11112; b) K.A. Peterson, D. Figgen, M. Dolg and H. Stoll, *J. Chem. Phys.*, 2007, **126**, 124101; c) D. Figgen, K.A. Peterson, M. Dolg and H. Stoll, *J. Chem. Phys.*, 2009, 130, 164108.

[S8] a) J.P. Foster and F. Weinhold, *J. Am. Chem. Soc.*, 1980, **102**, 7211-7218; b) F. Weinhold, *J. Comput. Chem.*, 2012, **33**, 2363-2379 and references therein. c) C.R. Landis and F. Weinhold, F. The NBO View of Chemical Bonding, in "*The Chemical Bond: Fundamental Aspects of Chemical Bonding*" (eds G. Frenking and S. Shaik), Wiley-VCH Verlag GmbH & Co. KGaA, Weinheim, Germany, 2014.

[S9] K.B. Wiberg, *Tetrahedron* 1968, **24**, 1083-1096.

.